Research Article

Biochemical Characterization of High Mercury Tolerance in a *Pseudomonas* Spp. Isolated from Industrial Effluent

Santosh Kumar Sahu[1]*, Himadri Gourav Behuria[1], Sangam Gupta[1],
Rubirekha B. Dalua[1], Susmita Sahoo[1], Debendra Parida[1],
Simarani Ghosh[1], and Subhasmita Padhi[1]

[1]Department of Biotechnology, North Orissa University, Baripada, Odisha, India

Abstract

A mercury resistant *Pseudomonas* spp. was isolated from industrial effluent that was able to tolerate 200 μM HgCl$_2$. The Hg^{2+}-resistant *Pseudomonas* spp. exhibited elevated stress-regulatory mechanisms as indicated by its high and inducible mercury reductase activity, high intrinsic catalase activity and enhanced resistance to Hg^{2+}-induced release of protein-bound iron. An enhanced resistance of the bacterium to Hg^{2+}-induced lipid peroxidation was observed as indicated by 40% lower conjugated diene and 60% lower lipid hydroperoxide content compared to a non-mercury resistant strain *Pseudomonas aeruginosa* (ATCC 27853). Phospholipid (PL) analysis of both the species reveled intrinsic differences in their PL composition. We observed 80% PE, 15% PG and 5% of an unidentified PL (U) in MRP compared to 65% PE, 20% PG and 17% CL in *Pseudomonas aeruginosa* (ATCC 27853). Mercury toxicity led to significant reorganization of PL in *Pseudomonas aeruginosa* (ATCC 27853) compared to MRP. While HgCl$_2$ led to 25% increase in PE, 35% depletion in CL and 27% depletion in PG content of *Pseudomonas aeruginosa* (ATCC 27853), MRP exhibited only 5% enhancement in PE content that was accompanied by 20% depletion in PG content, indicating that MRP resists mercury induced PL organization. Interaction of the MRP with polystyrene surface showed two fold higher Hg^{2+}-induced exopolysaccharide secretion and elevated biofilm forming ability compared to *Pseudomonas aeruginosa* (ATCC 27853). Our investigation reveals a novel *Pseudomonas* spp. with high Hg^{2+}-tolerance mechanisms that can be utilized for efficient bioremediation of mercury.

Competing Interests: The authors have declared that no competing interests exist.

*Correspondence to: Santosh Kumar Sahu, Department of Biotechnology, North Orissa University, Takatpur, Baripada, Odisha, India

Email: drsantoshnou@gmail.com

Introduction

Mercury (Hg) and its derivatives (e.g. Hg^{2+}, CH_3Hg, CH_3HgCH_3 etc.) are amongst the most hazardous environmental pollutants because of their toxicity, non-biodegradability and ability of bio-accumulation [1]. Most of the contaminating Hg comes from anthropogenic sources such as industrial activities and get deposited in soil and water bodies. Hg^{2+} is acutely toxic at nanomolar concentration, adversely affecting health and survival of plants, animals and microbes [2, 3]. In human, Hg has profound patho-physiologic toxicity at all concentrations [4]. Traditionally applied Hg removal processes that use ion-exchange or bio-sorbent technology, prove to be less effective and produce toxic byproducts [5]. Hence, it is essential to develop effective and eco-friendly Hg^{2+} bioremediation technologies using novel Hg^{2+} tolerant bacterial strains for detoxification of Hg and its derivatives from water and soil samples [6, 7]. However, the mechanism of Hg^{2+}-induced toxicity, Hg^{2+} tolerance and detoxification in bacteria remains elusive [8].

Hg^{2+}-induced cytotoxicity in bacteria and other life forms is mediated by enhanced oxidative stress as indicated by accumulation of oxidized DNA, lipid hydroperoxides (LHP) and oxidative damage of iron-sulfur (Fe-S) clusters of vital enzymes [9-11]. Hg^{2+}-resistant species are known to over express Mer operon including the enzyme mercuric reductase (MerA) that efficiently reduces more toxic ionic Hg^{2+} to less toxic and volatile metallic (Hg^0) form. Other Hg^{2+} tolerance mechanisms include acute regulation of cytosolic oxidative stress, regulation of cytosolic iron content, enhanced synthesis of Hg^{2+}-resistant biomolecules and biofilm formation. Formation of biofilms is a bacterial physiological response to survive the effect of toxic compounds in the environment that is mediated through enhanced production of extracellular polymeric substances (EPS) [12].

Lipids are among the most vulnerable group of biomolecules that are prone to oxidative damage by reactive oxygen species (ROS) produced in response to heavy metal toxicity. In *Pseudomonas aeruginosa*, three phospholipids (PLs), named phosphatidyl ethanolamine (PE), phosphatidyl glycerol (PG) and cardiolipin (CL) constitute ~ 90% of total cellular lipids [13]. However, variation in cellular PL composition is an adaptive response of bacteria to extreme environmental conditions such as osmotic stress, heavy metal ion toxicity and growth phase [14]. Oxidative damage to membrane lipids is known to alter lipid packing, fluidity and function of cell membrane including interaction of the cell with solid surfaces [15, 16]. Hence, bacteria may respond to Hg^{2+}-induced oxidative stress by acute regulation of PL composition in plasma membrane that affects its interaction with solid substrate.

We isolated a Hg^{2+}-resistant *Pseudomonas spp* (MRP) from industrial effluents and systematically investigated its cellular response to elevated Hg^{2+} compared to non-Hg^{2+}-resistant strain *Pseudomonas aeruginosa* (ATCC 27853). Our investigation identifies a novel Hg^{2+} tolerant *Pseudomonas* spp. with enhanced Hg^{2+}-reducing ability.

Materials and methods

Chemicals: PL standards: PC, PE, PG and CL were purchased from Sigma (India). Lysozyme, bovine serum albumin (BSA), Triton-X-100, $FeCl_3$, Ferrozine, Neucoproine, ammonium acetate,

ascorbic acid, ammonium molybdate, potassium permanganate, sodium hydroxide, sodium chloride, sodium carbonate, sodium potassium tartarate, copper sulphate, Tris Buffer and components of LB media (Yeast extract, Tryptone and Agar), Congo Red, were obtained from Himedia (India). $HgCl_2$, Silica gel GF 254, Follin's reagent and Iodine balls were purchased from Merck (India). Butylated Hydroxy Toluene (BHT) was obtained from Sisco Research Laboratory (SRL). All organic solvents (Chloroform, Methanol, Acetic acid, and Ammonia solution (25%), Acetone) were purchased from Merck (India). Inorganic acids: Hydrochloric acid and Perchloric acid were purchased from Merck (India). All routine chemicals were purchased from Himedia.

Bacterial strains, growth condition and determination of Hg^{2+} tolerance: The MRP was isolated from a pool used for dumping effluent from a soft drink manufacturing industry for last 27 years. *Pseudomonas aeruginosa* (ATCC 27853) was used as a control in all the experiments conducted on MRP. Both the strains were maintained in LB-agar plates. Hg^{2+} tolerance of the strains was determined by analyzing their growth in LB containing increasing concentration of $HgCl_2$. Growth of the strains were performed by inoculating 100 ml broth in 250 ml Erlenmeyer flask with 1 ml seed culture grown for 12 h at 25 ℃ and 200 rpm. OD_{600} of the cultures were measured each 2 h to quantitate the effect of Hg^{2+} on growth rate. The cells were grown to saturation phase at 25 ℃ and 200 rpm before collection. Cells were collected by centrifugation at 5000 $\times$ g for 7 min at 25 ℃ and resuspended at ~10 mg ml^{-1} in re-suspension buffer (RSB) (50 mM Tris-HCl, pH 7.5, 100 mM NaCl, 5 mM BHT) and used immediately for further experiments.

Protein estimation: Protein was quantitated by Lowry's method with modification [17]. Briefly, 16 μl of re-suspended cells was incubated with 10 μg lysozyme, followed by 1% (w/v) Triton-X-100 at 25 °C for 30 min. The whole cell lysate was mixed with Lowry's reagents (reagent I and II) in a final assay volume of 2.6 ml and incubated for 1 h at 25 ℃. The assay mix was centrifuged at 5000 $\times$ g and A_{750} of the supernatant was measured using a Systronics double beam spectrophotometer (Model 2202, Japan). Protein concentration in samples was calculated from the standard curve using 1mg ml^{-1} BSA.

Mercuric reductase (MR) assays: MR assays were performed following procedures of Fox and Walsh with modification [18]. Mid-log phase (OD = 0.6) cultures of *Pseudomonas aeruginosa* (ATCC 27853) and MRP in LB were induced with increasing concentration of $HgCl_2$ and grown at 25 ℃ for 6 h at 200 rpm. Cells were collected at 5000 g for 5 min at 4 ℃ and resuspended at 50 mg ml^{-1} in assay buffer (RSB containing 0.5 mM EDTA and 1 mM β-mercaptoethanol) and were incubated with 10 mg ml^{-1} lysozyme for 30' at 37 °C followed by brief sonication for 1 min at 4 °C using a probe sonicator (Thermo Scientific, India). MR assay was performed on cells containing 1 mg protein in assay buffer (50 mM Tris-HCl, pH 7.5, 100 mM NaCl, 1 mM β-mercaptoethanol, 200 μM NAD(P)H and 50 μM $HgCl_2$) in a final volume of 800 μl. Mercury-dependent NAD(P)H oxidation was monitored as the decrease in A_{340} using a Systronics double beam spectrophotometer (Model 2202, Japan). Initial rate of NAD(P)H oxidation was determined in the first 10s, when the A_{340} decreased linearly with time. Specific Hg-dependent NAD(P)H oxidation rate expressed as units mg $protein^{-1}$ [1 U = μmol of NAD(P)H oxidized min^{-1}] was calculated by subtracting the slope of the curves obtained in the absence of $HgCl_2$ from that observed following $HgCl_2$ addition.

Catalase assay: Catalase assay was performed on freshly collected cells using the method of Beers and Sizer [19]. Briefly, 2 mg cells were lysed by incubating sequentially with 0.5 mg lysozyme and

1% (w/v) in 1 ml RSB. The supernatant was collected after centrifuging the lysate at 10,000 $\times$ g for 5 min at 4 ℃. Catalase activity in the supernatant was quantitated by measuring the time dependent depletion of absorbance of H_2O_2 at 240 nm (A_{240}) in 3 ml assay mix (6.66 mM H_2O_2, 50 mM Tris-HCl, pH 7.5, 100 mM NaCl, and 0.3 ml cell lysate). The background absorbance due to protein in the assay mix was corrected by subtracting A_{240} of the assay mix without H_2O_2 from all the samples. Data obtained were analyzed by fitting to Michelis-Menten equation using Graph-pad prism (version 6).

Quantitation of cytosolic iron content: Cytosolic iron content was quantitated using methods described previously [20]. Briefly, 1mg cell in 0.2 ml resuspension buffer was lysed in 0.8 ml of 10 mM HCl and neutralized with 1 ml 50 mM NaOH. Protein-bound iron was released by adding 1 ml iron releasing reagent (IRR) (2.25% $KMnO_4$ in 0.7 M HCl) followed by incubation at 62 ℃ for 2 h. Iron thus released was detected using 0.3 ml iron-detection reagent (IDR) (6.5 mM ferrozine, 6.5 mM neocuproine, 2.5M ammonium acetate, and 1M ascorbic acid) followed by incubation at 25 ℃ for 30 min. Intensity of the purple color developed was quantitated by measuring A_{550} of the assay mix using a Systronics double beam spectrophotometer (Model 2202, Japan) and iron content was calculated from standard curve of $FeCl_3$.

Extraction of total lipid: Total lipid was extracted using aqueous two phase method of Bligh and Dyer [21]. Briefly, 1 mg cell in 0.5 ml RSB was mixed with 1.9 ml $CHCl_3$:CH_3OH (1:2 v/v) followed by 0.625 ml $CHCl_3$. Aqueous and organic phases were separated by adding 0.625 ml H_2O, mixed and centrifuged at 3000 $\times$ g at 25 ℃ in a table top Sorval (REMI, India). Lower phase was collected and upper phase was re-extracted with 0.625 ml $CHCl_3$. $CHCl_3$ was evaporated in the rotary evaporator over night at room temperature. The dried lipid samples were dissolved in $CHCl_3$ at approximately 100 μmol ml^{-1} PL and stored at -20 ℃.

Quantitation of PL content:

PL content in total lipid extract was quantitated by method of Fiske and Subarrow [22]. Briefly, dried lipid cake from 100 μl total lipid extract was completely dried and incubated with 325 μl of 11 M perchloric acid at 150 ℃ for 2 h. Samples were removed, diluted with 1.65 ml H_2O, added with 0.25 ml 2.5% (w/v) ammonium molybdate, followed by 0.25 ml 10% ascorbic acid and incubated at 100 ℃ for 10 min. Intensity of color developed was quantitated by measuring A_{797} of the samples using a Systronics double beam spectrophotometer (Model 2202, Japan) and compared with KH_2PO_4 standards (1 nmol $μl^{-1}$) to calculate total PL content.

Quantitation of conjugated-diene content from total lipid extract: Diene conjugation of lipids was quantitated following the procedures of Howlett and Avery with modification [23]. Briefly, lipid extract containing 1 μmol PL in $CHCl_3$ was dried in rotary evaporator overnight and the lipid cake was dissolved in 3 ml cyclohexane. Absorbance of the samples was scanned from 200 nm to 400 nm. Two peaks were observed at 230 nm (A_{230}) and 274 nm (A_{274}) respectively. The ratio A_{230}/A_{274} gives the relative amount of conjugated-dienes formed in the samples.

Quantitation of lipid hydroperoxide (LHP) content: LHP formed in total lipid extract was quantitated following the procedure of Fukuzawa et al. [24]. Briefly, 5 ml assay mix containing 100 μM xylenol orange, 3 μmol PL, 1 mg egg yolk PC (EYPC), 60% methanol, 1 mM BHT and 25 mM H_2SO_4 was sonicated using a probe sonicator at 40 ℃ for 30 min. 100 μM Fe^{2+} was added to the assay mix and incubated at 25 ℃ for 60 min to initiate the LHP-dependent conversion of Fe^{2+} to

Fe^{3+} that has an absorption maximum at 600 nm. A_{600} of the samples were recorded and compared to the untreated controls to calculate the relative amount of LHP formed as described previously.

Two dimensional thin layer chromatography (2D-TLC): 2D-TLC of total lipid extract was performed using methods described previously [25]. Lipid extract containing 500 nmol PL in 50 μl $CHCl_3$ was applied to a 20 cm × 20 cm × 0.0002 cm silica gel (GF 254) TLC plate (Merck, India). The samples were developed in first and second dimension using solvent I ($CHCl_3$:CH_3OH: 25% ammonia solution 65:35:5 by volume) and II ($CHCl_3$:C_3OH_6: CH_3OH:CH_3COOH:H_2O in 50:20:10:10:5 by volume) respectively. The plates were air dried and spots were detected using iodine vapor. The PLs were identified using PL standards developed in the same condition. The spots were scrapped into assay tubes for PL quantitation.

Quantitation of phospholipids from spots on TLC plates: Silica powder from the spots were scrapped into 12 × 125 mm glass assay tubes and their weight was determined. The powder was added to 400 μl perchloric acid (11 M) and incubated at 150 ℃ for 2 h. The released phosphate was quantitated following method of Fiske and Subarrow [22]. PL in each spot was calculated by subtracting the error originated from silica powder collected from unstained areas of TLC plates.

Asaay for biofilm formation on polystyrene plates: Biofilm forming ability of *Pseudomonas aeruginosa* (ATCC 27853) and MRP in response to Hg^{2+} toxicity was determined by microtiter plate assay as described previously [26]. Briefly, overnight (12h) culture of bacteria were diluted 100 fold with fresh LB containing increasing concentration of $HgCl_2$ and 100 μl of this diluted culture was transferred into the wells of microtiter plate and incubated for 72 h at 25 ℃. Biofilm developed in the well of the microtiter plate was stained with 0.1% (w/v) crystal violet, dried and solubilized with 125 μl 30% acetic acid. Intensity of color developed was quantitated by measuring A_{500} of the solubilized biofilm in a micro plate reader (Biorad).

Quantitation of EPS production: EPS production by the bacteria were quantitated using congored (CR) binding assay as described previously with modification [27]. Briefly, stationary phase cultures were adjusted to $OD_{600} = 10$ in 3 ml RSB (50 mM Tris-HCl, pH 7.5, 100 mM NaCl, 5 mM BHT), 40 mg L^{-1} CR was added and incubated for 1 h at 25 ℃. Cells were removed by centrifugation and the A_{490} of the supernatant was determined to quantitate the residual amount of CR in the solution.

Statistical Analysis: Statistical significance of data were evaluated by Student's "t" test for the biochemical studies and One-way ANOVA test was used to compare the results whenever more than two experimental groups were compared. All the data are expressed as Mean ± STDEV (standard deviation).

Results

MRP exhibits high Hg^{2+}-tolerance and inducible mercury reductase (MerA) activity: MRP exhibited growth in LB medium containing up to 200 μM $HgCl_2$, whereas the non-Hg^{2+}-resistant *Pseudomonas aeruginosa* (ATCC 27853) exhibited growth only up to 6 μM $HgCl_2$ (Fig. 1 A and B). No growth was observed in *Pseudomonas aeruginosa* (ATCC 27853) beyond 6 μM $HgCl_2$. In absence of $HgCl_2$, the MRP showed saturation at 14 h and the saturation time increased gradually up to 36 h at 200 μM $HgCl_2$. The slow growth rate was basically due to prolonged lag phase rather

than delayed log phase. Cells grown at all concentrations of Hg^{2+} exhibited equal total protein content at saturation phase (data not shown). We observed high mercuric reductase (MerA) activity in MRP compared to *Pseudomonas aeruginosa* (ATCC 27853) (Fig. 1 C and D). MRP showed 12 mU mg^{-1} MerA activity in LB that increased up to 45 mU mg^{-1} in presence of 200 μM $HgCl_2$. These results indicate that $HgCl_2$ induces high MerA activity in MRP. However, *Pseudomonas aeruginosa* (ATCC 27853) exhibited low (3 mU mg^{-1}) MerA activity that remained unchanged with increasing $HgCl_2$ up to 6 μM. Our results show that MRP possess high mercury tolerance with inducible MerA activity.
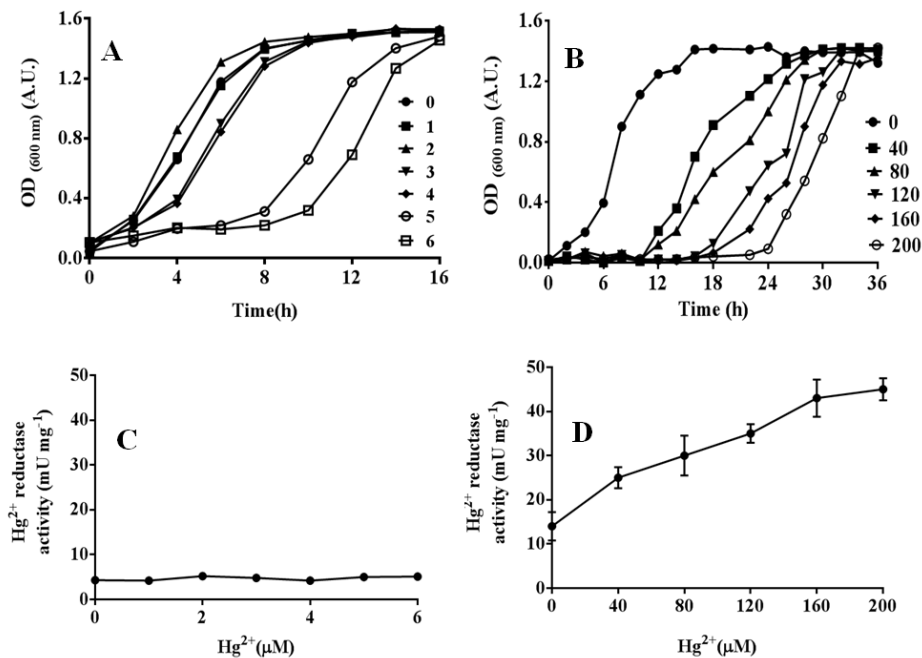

Fig. 1 Growth curves of (A) *Pseudomonas aeruginosa* (ATCC 27853) and (B) MRP in LB containing increasing concentration of $HgCl_2$ as indicated on the right of the. Mercury reductase activity of (C) *Pseudomonas aeruginosa* (ATCC 27853) and (D) Hg^{2+}-resistant MRP in LB containing increasing concentration of $HgCl_2$ as indicated on the right of the. Data presented here show the mean ±standard daviation (n=4).

MRP exhibits enhanced oxidative stress regulatory mechanisms: As Hg^{2+} is known to enhance oxidative stress in different cell types and catalase is the central oxidative stress regulatory enzyme in bacteria, we quantitated the catalase activity in MRP and *Pseudomonas aeruginosa* (ATCC 27853) in response to $HgCl_2$-induced toxicity. MRP exhibited high intrinsic catalase activity as indicated by its 25 folds higher degradation rate of H_2O_2 compared to *Pseudomonas aeruginosa* (ATCC 27853) (Fig. 2 A and B). Presence of 6 μM $HgCl_2$ in growth medium enhanced catalase activity by 15 folds in *Pseudomonas aeruginosa*, where as the catalase activity of MRP remained almost unchanged in presence of 200 μM $HgCl_2$. Our results show that Hg^{2+} enhances oxidative stress in *Pseudomonas aeruginosa* (ATCC 27853), where as MRP resists Hg^{2+}-induced oxidative stress by its high intrinsic catalase activity [26].
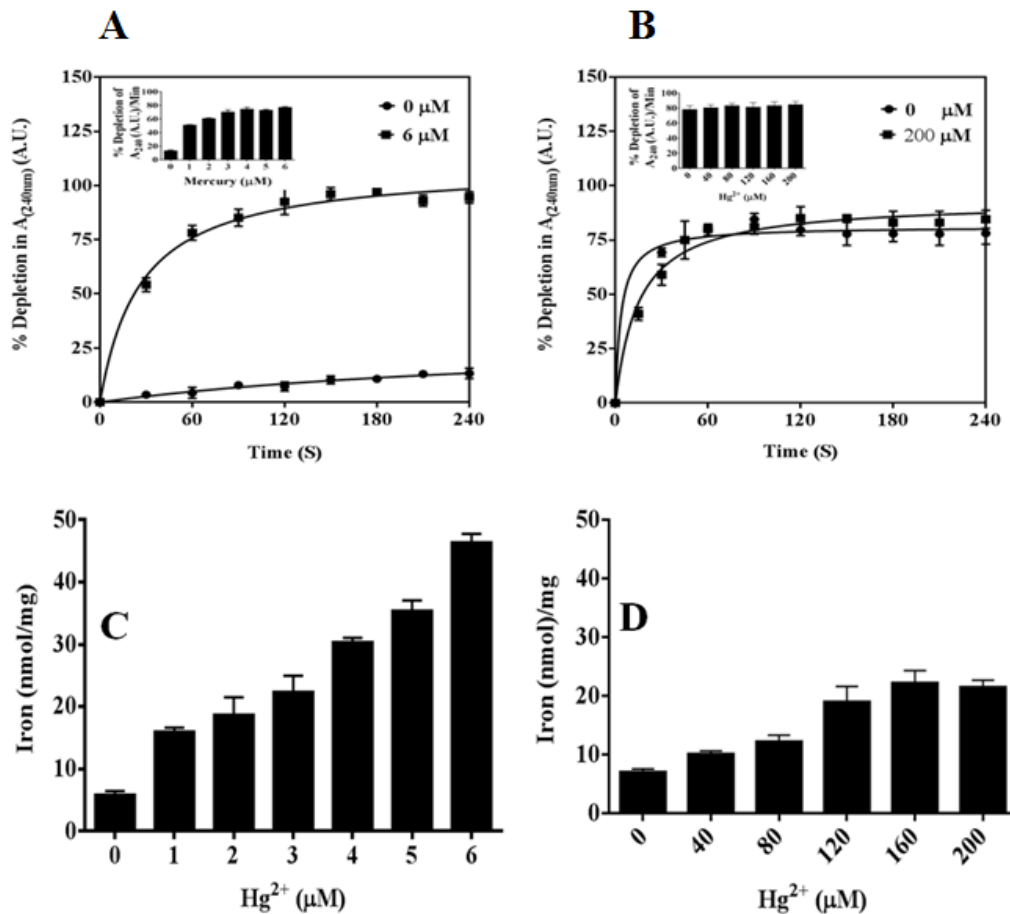
Fig. 2 Oxidative stress induced by *Pseudomonas aeruginosa* (ATCC 27853) and MRP grown in LB in presence or absence of Hg^{2+} as indicated in the figures. Catalase activity of (A) *Pseudomonas aeruginosa* (ATCC 27853) and (B) MRP. The inset shows the dose-dependence of catalse activities on concentration of $HgCl_2$ in the growth medium. Effect of $HgCl_2$ on cytosolic iron content of (C) *Pseudomonas aeruginosa* (ATCC 27853) and (D) MRP. Data presented here show the mean ±standard daviation (n=4).

Recent investigation shows profound effect of oxidative stress on free cytosolic iron content [27, 28]. Hence, we analyzed cytosolic iron content in *Pseudomonas aeruginosa* (ATCC 27853) and MRP when grown in presence of increasing $HgCl_2$. Our results show that in *Pseudomonas aeruginosa* (ATCC 27853), cytosolic iron content was augmented by 30-40% when grown in presence of 4 µM of $HgCl_2$ and increased rapidly (up to 5 folds) in response to 5-6 µM Hg^{2+} (Fig 2 C). However, MRP showed only 2.5 fold (20 nmols) increase in cytosolic iron content (Fig 2D). These results show that MRP resisted Hg^{2+}-induced release of protein-bound iron into the cytosol compared to *Pseudomonas aeruginosa* (ATCC 27853).

MRP resists Hg^{2+}-induced lipid peroxidation: Both the bacterial strains used in the experiments exhibited ~125 nmol PLs mg^{-1} of total protein that remained unchanged in presence of Hg^{2+} (data

not shown). However, in *Pseudomonas aeruginosa* (ATCC 27853), conjugated diene, a product of early lipid peroxidation quantitated by A_{228}/A_{274} was gradually augmented to 165% in presence of 4 μM $HgCl_2$, accompanied by slow increase in lipid hydroperoxide (LHP) content by 20% of un treated controls (Fig. 3A and C). However, beyond this concentration, conjugated diene content was depleted to 120% accompanied by rapid increase in LHP content by 3.5 fold. These results show that $[Hg^{2+}] \geq 4$ μM leads to oxidation of lipids at a faster rate, resulting in quick conversion of conjugated dienes into LHP. In contrast, MRP resisted Hg^{2+}-induced lipid peroxidation as shown by only 20% enhancement in conjugated diene content and 25% enhancement in LHP content in presence of 200 μM $HgCl_2$ (Fig. 3 B and D). These results show that MRP exhibits enhanced resistance to Hg^{2+}-induced lipid peroxidation [23].
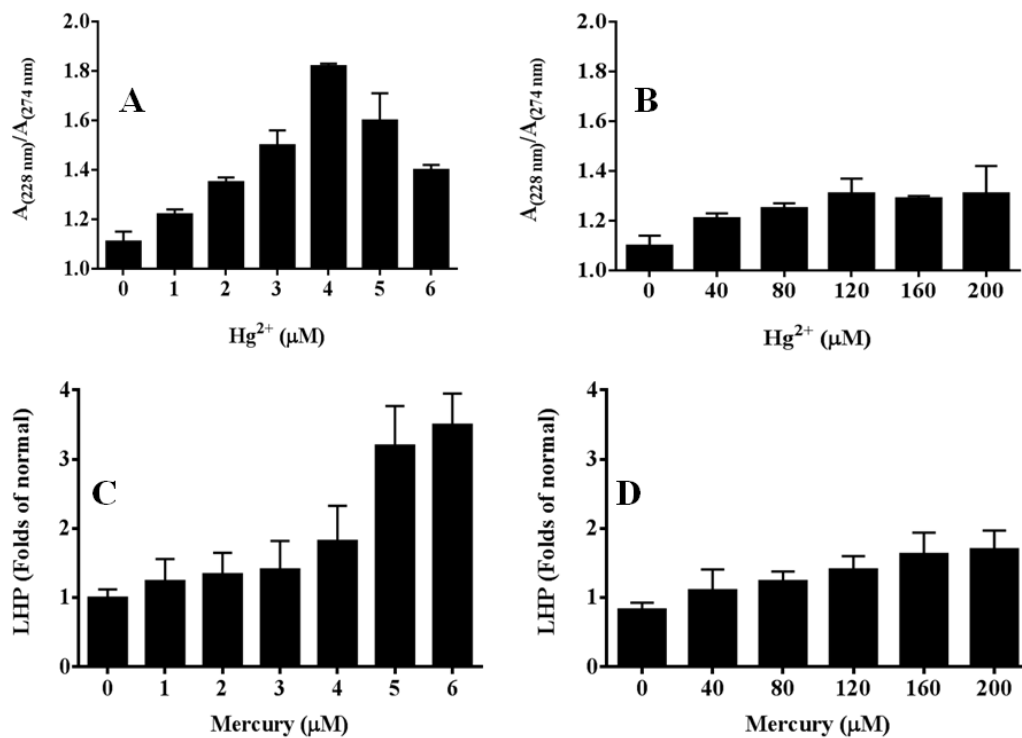

Fig. 3 Analysis of lipid peroxidation induced by Hg^{2+} in *Pseudomonas aeruginosa* (ATCC 27853) and MRP. Relative amount of conjugated diene content in (A) *Pseudomonas aeruginosa* (ATCC 27853) and (B) MRP induced by Hg^{2+} toxicity. Relative amount of lipid hydroperoxide (LPH) content in (C) *Pseudomonas aeruginosa* (ATCC 27853) and (D) MRP induced by Hg^{2+} toxicity. The results presented show mean ±standard daviation (n=4).

MRP exhibited altered PL composition compared to *Pseudomonas aeruginosa* (ATCC 27853): PL constitute ~90% of total lipid in MRP that shows compositional variation in response to extreme environmental conditions such as ionic stress and heavy metal toxicity. Hence, we performed a quantitative analysis of cellular PL composition in *Pseudomonas aeruginosa* (ATCC 27853) and MRP to investigate the effect of Hg^{2+} on cellular PL composition. In *Pseudomonas aeruginosa* (ATCC 27853), PE, PG and CL constituted 63%, 20% and 17% of total PL respectively (Fig. 4 A).

Increasing doses of Hg^{2+} up to 6 μM led to augmentation of PE to 75% of total PL, accompanied by gradual depletion of PG and CL to 15% and 12% respectively. However, MRP exhibited 80% PE and 15% PG. No CL was detected in MRP (Fig. 4 B). Hg^{2+}-induced toxicity led to increase in PE up to 85% and depletion of PG to 12%. In addition, an unidentified PL (U) was observed that didn't show significant variation in response to Hg^{2+}-toxicity. Our results show that MRP exhibited enhanced resistance to Hg^{2+}-induced alteration in PL compotition compared to *Pseudomonas aeruginosa* (ATCC 27853).
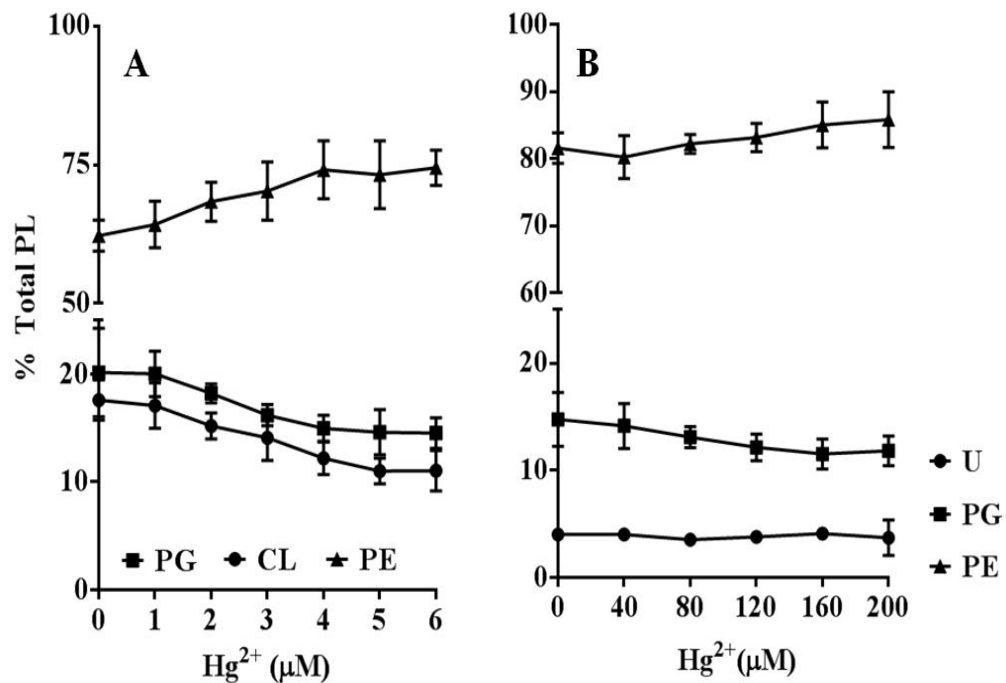

Fig. 4 Effect of Hg^{2+} on PL composition of *Pseudomonas aeruginosa* (ATCC 27853) and MRP. Dose dependence of (A) PE, PG and CL of *Pseudomonas aeruginosa* , (B)   PE, PG and U   of   MRP on $HgCl_2$ in growth medium . The results presented show mean ± standard daviation (n=4).

MRP exhibits enhanced EPS secretion and biofilm forming ability in response to Hg^{2+}: Enhanced secretion of EPS and formation of biofilm are important physiological adaptations by bacteria to survive heavy metal toxicity [26, 29]. Hence, we investigated formation of EPS and biofilms in *Pseudomonas aeruginosa* (ATCC 27853) and MRP in response to Hg^{2+} toxicity. Our results show that EPS production gradually increased by 20% and 30% in *Pseudomonas aeruginosa* (ATCC 27853) and MRP respectively in response to 6 and 200 μM Hg^{2+} (Fig. 5 A and B). We observed a slow rate of Hg^{2+}-induced EPS secretion in *Pseudomonas aeruginosa* (ATCC 27853). However, a rapid production of EPS was observed in MRP up to 80 μM Hg^{2+} that remained invariable up to 200 μM $HgCl_2$.
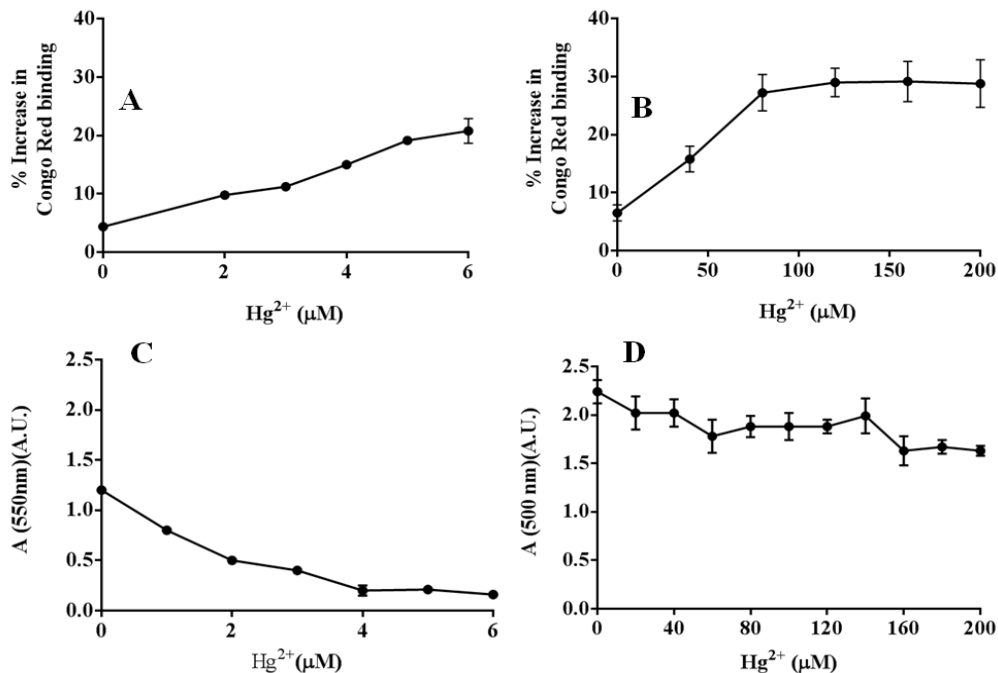
Fig. 5 Effect of Hg^{2+} on interaction of *Pseudomonas aeruginosa* (ATCC 27853) and MRP on solid substrates. Effect of Hg^{2+} on secretion of EPS in (A) *Pseudomonas aeruginosa* (ATCC 27853) and (B) MRP. Effect of Hg^{2+} on relative amount of biofilm formation of (C) *Pseudomonas aeruginosa* (ATCC 27853) and (D) MRP on polystyrene substrates. Results presented here show mean ± standard daviation (n=4). Significance of the results were verified by Student's t test (P = 0.05) using Graphpad prism (version 6).

Biofilm forming ability of MRP was 2 fold higher compared to *Pseudomonas aeruginosa* (ATCC 27853) on polystyrene surface. Increase of HgCl$_2$ in growth medium up to 6 μM almost abolished the ability of biofilm formation in *Pseudomonas aeruginosa* (ATCC 27853). However, the Biofilm of MRP remained almost unaffected up to 200 μM HgCl$_2$. Our results show that MRP possess high EPS and biofilm forming ability compared to *Pseudomonas aeruginosa* (ATCC 27853) that constitutes one of its primary mechanisms of its high Hg^{2+} resistance.

Discussion

In the present work, we investigated in part, the mechanism of Hg^{2+} resistance in a MRP and compared it with a non Hg^{2+}-resistant soil bacterium *Pseudomonas aeruginosa* (ATCC 27853). Our investigation showed (i) enhanced Hg^{2+} reductase activity, (ii) enhanced oxidative stress regulatory mechanisms (iii) higher resistance to Hg^{2+}-induced lipid peroxidation, (iv) altered PL composition and (v) High EPS and biofilm forming ability in MRP compared to *Pseudomonas aeruginosa* (ATCC 27853).

Hg^{2+}-induced cytotoxicity reduced growth rate of MRP by increasing the lag phase indicating that prolonged lag phase is required for MRP to adapt to Hg^{2+}-induced toxicity. MerA is

the most important component of Mer operon that is known to be up regulated in response to Hg^{2+}-toxicity [30]. Our results show that MerA is upregulated in MRP in response to $HgCl_2$ by 4 folds. This enhanced MerA activity leads to rapid detoxification of Hg^{2+} and hence, enables survival of MRP in growth medium containing up to 200 μM $HgCl_2$ (Fig. 1 A-D).

MRP exhibited enhanced oxidative stress regulatory mechanisms as indicated by (i) high catalase activity and (ii) elevated resistance to release of protein-bound iron content compared to *Pseudomonas aeruginosa* (ATCC 27853) (Fig. 2 A-D). Catalase is the central oxidative stress regulatory enzyme that maintains minimal cytosolic concentration of reactive oxygen species (ROS). Catalase from different cell types increases in response to oxidative stress [31, 32]. Increase of catalase activity in *Pseudomonas aeruginosa* (ATCC 27853) in response to Hg^{2+} may be explained by assuming enhanced formation of cytosolic ROS (e.g. H_2O_2, $OH^{\bullet}$ and $O_2^{\bullet}$) like other heavy metals that enhances the cytosolic catalase activity [33-35]. Our results show that MRP exhibits intrinsically high oxidative stress regulatory mechanism as indicated by higher catalase activity. 200 μM Hg^{2+} slightly enhanced the catalase activity in MRP.

Cytosolic iron content increased by 10 fold in *Pseudomonas aeruginosa* (ATCC 27853) in response to 6 μM Hg^{2+}. However, only a 3 fold enhancement of cytosolic iron content was observed in MRP at 200 μM Hg^{2+}. These results show that MRP resists Hg^{2+}-induced release of cytosolic iron content. Hg^{2+} is known to tightly associate with iron-sulfur (4Fe-4S) clusters of multiple enzymes and proteins (e.g. fumarase) with exposed iron-sulfur clusters [11]. Hg^{2+} is known to increase production of cytosolic ROS that destroys the iron-sulfur (FeS) centers of multiple proteins, hence, releasing the bound iron [28, 36]. Our results show that MRP resists Hg^{2+}-induced destruction of FeS centers of enzymes indicating stringent regulation of cytosolic Hg^{2+} content.

Heavy metal-induced oxidative damage to cellular lipids is one of the primary mechanism of metal-induced cytotoxicity [23]. Our results show that MRP exhibits more resistance to Hg^{2+}-induced lipid peroxidation compared to *Pseudomonas aeruginosa* (ATCC 27853) that is indicated by lesser diene conjugation and LHP content (Fig. 3 A-D). Conjugated diene is one of the initial products of lipid peroxidation that is finally converted into LHP, the terminal form of oxidized lipid. Oxidation of lipids is known to detrimentally affect membrane integrity, energy producing efficiency, interaction with solid substrates (e.g. biofilm formation) and cell survival. Our results show that resistance to lipid peroxidation is one of the primary mechanisms by which MRP exhibits high tolerance to Hg^{2+}-induced toxicity.

PLs constitute the most important building block of plasma membrane that regulates function of multiple membrane-bound proteins and mediates microbial interaction with solid substrates [37]. Hence, we analyzed the effect of Hg^{2+} on PL composition of *Pseudomonas aeruginosa* (ATCC 27853) and MRP. We observed negligible CL content in MRP, 80% PE and 5% U. While, *Pseudomonas aeruginosa* (ATCC 27853) exhibited significant reorganization of its PLs as indicated by 25% increase in PE, 35% depletion in CL and 27% depletion in PG, MRP exhibited only 5% enhancement in PE content that was accompanied by 20% depletion in PG content. Our results show that MRP shows high resistance to Hg^{2+}-induced alteration in cellular PL composition (Fig. 4 A-B). CL is known to be the most vulnerable class of PLs that is prone to oxidative damage by cytosolic ROS content [38]. Our results show that MRP exhibits high resistance to Hg^{2+}-induced lipid peroxidation by depleting CL content and enhancing PE content.

Secretion of EPS and formation of biofilm on solid substrates are primary mechanisms of heavy metal tolerance in many bacteria [26]. We investigated interaction of *Pseudomonas aeruginosa* (ATCC 27853) and MRP with polystyrene surfaces (Fig. 5 A-D). Both *P. aeruginosa* and MRP responded to Hg^{2+}-induced cytotoxicity by enhancing EPS production by 15% and 25% respectively. However, MRP exhibited high biofilm forming ability compared to *Pseudomonas aeruginosa* (ATCC 27853) that remained almost unaltered in response to 200 μM $HgCl_2$. EPS plays an important role in removal of heavy metals from environment due to their involvement in flocculation, binding metal ions from solutions, encasing the cells and retarding their diffusion into the cells [29]. It also plays an important role in bacterial attachment to solid substrate, allows communication within bacterial population and enables horizontal transfer of genes among a population, leading to biofilm formation [39]. Our results show that MRP exhibits high Hg^{2+} tolerance by elevated secretion of EPS and enhanced ability of biofilm formation.

Conclusion

In conclusion, our investigation shows a novel Hg^{2+} resistant MRP and explains in part its mechanism of high Hg^{2+} tolerance. This strain will be highly useful in bacterial bioremediation of Hg^{2+}-contaminated water and soil samples.

Acknowledgements

References

1. Cardoso PG, Pereira E, Duarte AC, Azeiteiro UM. Temporal characterization of mercury accumulation at different trophic levels and implications for metal bio-magnification along a coastal food web. *Mar Pollut Bull.* 2014, 87:39-47
2. Deng C, Zhang D, Pan X, Chang F, Wang S. Toxic effects of mercury on PSI and PSII activities, membrane potential and transthylakoid proton gradient in *Microsorium pteropus*. *J Photochem Photobiol B*. 2013, 127:1-7
3. Tazisong IA, Senwo ZN, Williams MI. Mercury speciation and effects on soil microbial activities. *J Environ Sci Health A Tox Hazard Subst Environ Eng.* 2012, 47:854-62
4. Rice KM, Walker EM, Jr Wu M, Gillette C. Environmental mercury and its toxic effects. *J Prev Med Public Health.* 2014, 47:74-83
5. Selin NE. Science and strategies to reduce mercury risks: a critical review. *J Environ Monit.* 2011, 13:2389-2399
6. Chang JS, Hong J. Biosorption of mercury by the inactivated cells of *Pseudomonas aeruginosa* PU 21 (Rip64). *Biotechnol Bioeng.* 1994, 44:999-1006

7. Chen S, Wilson DB. Construction and characterization of *Escherichia coli* genetically engineered for bioremediation of Hg^{2+}-contaminated environments. ***Appl Env Microbiol.*** 1997, 63:2442-2445

8. Summers AO. Damage control: regulating defenses against toxic metals and metalloids. ***Curr Opin Microbiol.*** 2009, 12:138-144

9. Valko M, Morris H, Cronin MTD. Metals, toxicity, and oxidative stress. ***Curr. Med Chem.*** 2005, 12:1161-1208

10. Elbaz A, Wei YY, Meng Q, Zheng Q, Yang ZM. Mercury-induced oxidative stress and impact on antioxidant enzymes in *Chlamydomonas reinhardtii*. ***Ecotoxicology.*** 2010, 19:1285-93

11. Xu FF, Imlay JA. Silver (I), mercury (II), cadmium (II), and zinc(II) target exposed enzymic iron-sulfur clusters when they toxify *Escherichia coli*. ***Appl Environ Microbiol.*** 2012, 78:3614-3621

12. Singh R, Paul D, Jain RK. Biofilms: implications in bioremediation. ***Trends Microbiol.*** 2006, 14:389-397

13. Conrad RS, Gilleland HE (Jr). Lipid alterations in cell envelopes of polymyxin-resistant *Pseudomonas aeruginosa* isolates. ***J Bacteriol.*** 1981, 148:487-97

14. Schniederberend M, Zimmann P, Bogdanov M, Dowhan W , Altendorf K. Influence of K^+-dependent membrane lipid composition on the expression of the *kdp*FABC operon in *Escherichia coli*. ***Biochim Biophys Acta.*** 2010, 1798:32-48

15. Barak I, Muchova K. The role of lipid domains in bacterial cell processes. ***Int J Mol Sci.*** 2013, 14:4050-4065

16. Hoch FL. Cardiolipins and biomembrane function. ***Biochim Biophys Acta.*** 1992, 113:71-133

17. Lowry OH, Rosebrough NJ, Farr AL, Randall RJ. Protein measurement with the Folin phenol reagent. ***J Biol Chem.*** 1951, 193:265-75

18. Fox B, Walsh CT. Purification and characterization of a transposon-encoded flavoprotein containing an oxidation-reduction-active disulfide. ***J Biol Chem.*** 1982, 257:2498-2503

19. Beers RF, Sizer IW. Spectrophotometric method for measuring the breakdown of hydrogen peroxide by catalase. ***J Biol Chem.*** 1952, 795:133-140

20. Reimer J, Hoepken HH, Czerwinska H, Robinson SR , Dringen R. Colorimetric ferrozine based assay for the quantitation of iron in cultured cells. ***Anal Biochem.*** 2004, 331:370-375

21. Bligh EG, Dyer WJ. A rapid method for total lipid extraction and purification. ***Can J Biochem Physiol.*** 1959, 37:911-917

22. Fiske C, Subarrow Y. The colorimetric determination of phosphorous. ***J Biol Chem.*** 1925, 66:375-400

23. Howlett NG, Avery S. Induction of lipid peroxidation during heavy metal stress in *Saccharomyces cerevisiae* and influence of plasma membrane fatty acid unsaturation. ***Appl Env Microbiol.*** 1997, 63:2971-2976

24. Fukuzawa K, Fujisaki A, Akai K, Tokumura A, Terao J, Gebicki JM. Measurement of phosphatidylcholine hydroperoxides in solution and in intact membranes by the ferric–xylenol orange assay. ***Anal Biochem.*** 2006, 359:18-25

25. Schneiter R, Daum G. Analysis of yeast lipids. ***Methods Mol Biol.*** *2006,* 313:75-84

26. Ma L, Jackson KD, Landry RM, Parsek MR, Wozniak DJ. Analysis of *Pseudomonas aeruginosa* conditional Psl variants reveals roles for the Psl polysaccharide in adhesion and maintaining biofilm structure postattachment. ***J Bacteriol.*** 2006, 188:8213-8221

27. Willekens H, Chamnongpol S, Davey M, Schraudner M , Langebartels C, Montagu MV, Inze D, Camp WV. Catalase is a sink for H_2O_2 and is indispensable for stress defence in C3 plants. ***EMBO J.*** 1997, 16:4806-4816

28. Liochev SL. The role of iron-sulfur clusters in *in vivo* hydroxyl radical production**. *Free Radic Res.*** 1996, 25:369-84

29. Singh P, Cameotra SS. Enhancement of metal bioremediation by use of microbial surfactants. ***Biochem. Biophys Res Commun.*** 2004, 319:291-297

30. Giovanella P, Cabral L, Bento FM, Gianello C, Camargo FA. Mercury (II) removal by resistant bacterial isolates and mercuric (II) reductase activity in a new strain of *MRP* B50A. ***N Biotechnol.*** 2016, 33:216-23

31. Boujbiha MA, Hamden K, Guermazi F, Bouslama A, Omezzine A, Kammoun A, El Feki A. Testicular toxicity in mercuric chloride treated rats: association with oxidative stress. ***Reprod Toxicol.*** 2009, 28:81-89

32. Kobal AB, Horvat M, Prezelj M, Briski AS, Krsnik M, Dizdarevic T, Mazej D, Falnoga I, Stibilj V, Arneric N, Kobal D, Osredkar J. The impact of long-term past exposure to elemental mercury on antioxidative capacity and lipid peroxidation in mercury miners. ***J Trace Elem Med Biol.*** 2004, 17:261-74

33. Fenton HJH. Oxidation of tartaric acid in presence of iron**. *J Chem SOC.*** 1894, 65:899-910

34. Haber F, Weiss JJ. The catalytic decomposition of hydrogen peroxide by iron salts. ***Proc R SOC London Ser A.*** 1934, 147:332- 35

35. Westwater J, McLaren NF, Dormer UH, Jamieson DJ. The adaptive response of *Saccharomyces cerevisiae* to mercury exposure. ***Yeast.*** 2002, 19:233-239

36. Djaman O, Outten, FW, Imlay JA. Repair of oxidized iron-sulfur clusters in *Escherichia coli*. ***J Biol Chem.*** 2004, 279:44590-44599

37. Hazel JR, Williams EE. The role of alterations in membrane lipid composition in enabling physiological adaptation of organisms to their physical environment. ***Prog Lipid Res.*** 1990, 29:167-227

38. Lewis RNAH, McElhaney RN. The physicochemical properties of cardiolipin bilayers and cardiolipin-containing lipid membranes. ***Biochim Biophys Acta.*** 2009, 1788:2069-2079

39. Teitzel GM, Parsek M.R. Heavy metal resistance of biofilm and planktonic *Pseudomonas aeruginosa*. ***Appl Environ Microbiol***. 2003, 69:2313-2320